HAL
open science

Study of the combustion efficiency of polymers using a pyrolysis–combustion flow calorimeter

Rodolphe Sonnier, Belkacem Otazaghine, Laurent Ferry, J. Lopez-Cuesta

To cite this version:

Rodolphe Sonnier, Belkacem Otazaghine, Laurent Ferry, J. Lopez-Cuesta. Study of the combustion efficiency of polymers using a pyrolysis–combustion flow calorimeter. Combustion and Flame, 2013, 160 (10), pp.2182-2193. 10.1016/j.combustflame.2013.04.009 . hal-03272316

HAL Id: hal-03272316

https://imt-mines-ales.hal.science/hal-03272316v1

Submitted on 9 Jul 2021

HAL is a multi-disciplinary open access archive for the deposit and dissemination of scientific research documents, whether they are published or not. The documents may come from teaching and research institutions in France or abroad, or from public or private research centers.

L'archive ouverte pluridisciplinaire **HAL**, est destinée au dépôt et à la diffusion de documents scientifiques de niveau recherche, publiés ou non, émanant des établissements d'enseignement et de recherche français ou étrangers, des laboratoires publics ou privés.

Study of the combustion efficiency of polymers using a pyrolysis–combustion flow calorimeter

Rodolphe Sonnier *, Belkacem Otazaghine, Laurent Ferry, José-Marie Lopez-Cuesta

CMGD Material Center, Ecole des Mines d'Alès, 6, Avenue de Clavières, 30100 Alès, France

A B S T R A C T

The combustion efficiency of various polymeric materials was studied using a pyrolysis–combustion flow calorimeter (PCFC). Decreasing the combustion temperature in a PCFC leads to partial combustion and lower heat release rates. Combustion efficiency versus combustion temperature was modeled using a phenomenological equation and model parameters were related to the chemical structures of eight pure polymers. The flame inhibition effect was evaluated for two classical approaches in flame retardancy by plotting the combustion efficiency versus the combustion temperature. In the first one (the reactive approach), polystyrenes with different chemical groups substituted on the aromatic ring were studied. In the second one (the additive approach), three well-known flame retardants were incorporated into an ABS matrix: ammonium polyphosphate, tetrabromobisphenol A (TBBA), and a TBBA/antimony trioxide system. Results confirm the flame inhibition effect of halogenated compounds in both approaches. Finally, a correlation between peaks of heat release rate (pHRR) in a cone calorimeter and in a PCFC was attempted. Predicting pHRR in a cone calorimeter using a PCFC appears possible when no barrier effect is expected, if PCFC tests are carried out at a precise combustion temperature, for which the combustion efficiencies in both tests are the same.

Keywords:
PCFC
Cone calorimeter
Flame inhibition
Combustion efficiency
Flame retardancy

1. Introduction

When exposed to an intense heat source, polymers undergo thermal or thermo-oxidative decomposition, leading to release of highly combustible gases. The complete combustion of these gases in the presence of oxygen releases heat, water, and carbon dioxide if the polymer contains only C, H, and O atoms. Nevertheless, combustion is generally only partial and released heat is lower than expected. Combustion efficiency is calculated as the ratio of the real heat release to the maximum heat release (i.e., when combustion is complete).

The main mode of action of halogenated flame retardants is flame inhibition, i.e., the decrease in combustion efficiency. Flame inhibition is partly due to physical effects (dilution and heat capacity, which lead to the cooling of the flame) and partly due to chemical effects (scavenging of highly reactive radicals $H^{\cdot}$, $OH^{\cdot}$ that attack the hydrocarbons [1–3]). Halogenated molecules (such as HBr) react in the gaseous phase by trapping reactive radicals to give less reactive radicals [1]:

$$RX \rightarrow R^{\circ} + X^{\circ} \ (X = \text{Br or Cl}) \quad (1)$$

$$X^{\circ} + RH \rightarrow R^{\circ} + HX$$

$$HX + H^{\circ} \rightarrow H_2 + X^{\circ}$$

$$HX + OH^{\circ} \rightarrow H_2O + X^{\circ}.$$

Therefore, some combustible molecules are not fully oxidized, CO is produced (rather than CO_2), and the heat release is significantly reduced. The efficiency of various compounds in flame inhibition was estimated experimentally or by calculations [1–4]. This efficiency is mainly dependent on specific atoms. Metallic compounds containing Fe, Pb, or Cr are the most effective [1]. Intrinsic inhibition indices were calculated using a Van Krevelen approach for different atoms: C, H, F, Cl, Br, and I. The last two were found to be the most effective [3]. It was highlighted that CF_3Br and CF_3I inhibit flame by chemical action, while other studied additives (fluorinated additives) act mainly through physical effects. Some phosphorus flame retardants could also have a similar action, but their main mode of action is generally considered as char promotion in the condensed phase. Another important characteristic for an efficient flame inhibitor is its ability to be regenerated during the combustion process [2,3].

The pyrolysis–combustion flow calorimeter (PCFC) is an apparatus developed approximately 12 years ago to measure some important flammability parameters of polymers through nonflaming combustion [5]. Since it needs only milligrams of material, it is a powerful method for studying polymers synthesized in the laboratory in small amounts. Some research teams attempted to use

* Corresponding author.
E-mail address: rodolphe.sonnier@mines-ales.fr (R. Sonnier).

PCFC as a screening tool before performing cone calorimeter tests, which need a greater amount of material [6–8]. But the correlation between the cone calorimeter and the PCFC results is not general, for three main reasons [9]. The first is the barrier effect, which is not efficient in the PCFC, in contrast to the cone calorimeter. The barrier effect becomes effective when an insulating layer could protect the underlying material from the heat source. This layer may be composed of char and/or mineral particles and should be thermally stable. The second is related to thermal stability. Two polymers could exhibit similar peaks of heat release rate but different degradation temperatures in PCFC. In this case, cone calorimeter results could be very different. The third reason is that the combustion is complete in the PCFC standard test while the combustion efficiency could be less than 1 in the cone calorimeter test, even if this test is carried out under well-ventilated conditions.

Nevertheless, it is possible to monitor the conditions (oxygen rate and temperature) in the PCFC combustion chamber to decrease the combustion efficiency, as presented in an article of Schartel et al. [10]. The decoupling between pyrolysis and combustion in the PCFC allows changing the conditions of combustion without modifying the pyrolysis of the sample. This possibility should allow studying the flame inhibition of halogenated flame retardants. But to the best of our knowledge, this possibility has never been exploited. We believe that only the chemical component of flame inhibition could be studied, since the combustion temperature is kept fixed during the test.

In the present article, the combustion temperature in the PCFC was monitored to study the change in combustion efficiency for various polymeric materials. This method was developed to know the role of different elements (Cl, Br, P) as efficient flame retar-

Table 1
Chemical composition of the materials studied.

Series	Designation	Name	Chemical structure
A	PS	Polystyrene	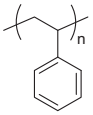
	PS-CH_3	Poly(4-methylstyrene)	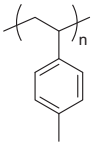
	PS-OCH_3	Poly(4-methoxystyrene)	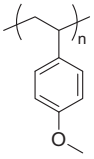
	PS-Cl	Poly(4-chlorostyrene)	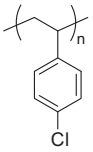
	PS-Br	Poly(4-bromostyrene)	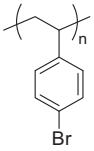
	PS-P	Poly(diethyl vinylbenzylphosphonate)	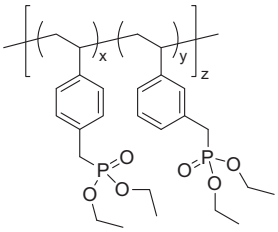
B	LDPE	Riblene FL20 (Polimeri Europa)	
	PMMA	Altuglas V825T (Arkema)	
	PS	Lacqrene 1340 (Arkema)	
	ABS	Terluran GP22 (BASF)	
	PA6	Technyl C216 (Rhodia)	
	PA11	Rilsan (Arkema)	
	EVA (28 wt% vinyl acetate)	Evatane 2805 (Arkema)	
	PVC	EVC Compound	
			FR content (wt%)
C	ABS + APP	Terluran GP22 (BASF) + AP423 (CLARIANT)	3.1, 7.9, 15.7, 31.5, 40
	ABS + TBBA	Terluran GP22 (BASF) + tetrabromobisphenol A	1.6, 15.6, 31
	ABS + TBBA/Sb_2O_3	Terluran GP22 (BASF) + tetrabromobisphenol A/antimony trioxide	1.7/0.6, 4.2/1.5, 8.5/3, 13.6/4.8, 18.6/6.6

dants. Two classical approaches in flame retardancy were studied: The first is the reactive approach, where flame retardant groups are grafted onto the macromolecular backbone. The second is the additive approach, where flame retardant compounds are physically incorporated into the polymer. Finally, an attempt was made to predict the combustion efficiency in the cone calorimeter from PCFC results.

2. Experimental

Three series of materials were studied (listed in Table 1). Series A gathers polystyrenes with various substituent groups in the *para* position on phenyl rings. Polystyrene is Lacqrene 1340. Poly-(4-methylstyrene, 4-methoxystyrene, 4-chlorostyrene, or 4-bromostyrene) is provided by Aldrich. Poly(diethyl vinylbenzylphosphonate) was synthesized in the laboratory. For this polymer, the substituent group is partially in the *meta* and partially in the *para* position. Series B gathers various pure commercial polymers. Series C gathers acrylonitrile butadiene styrene (ABS) polymers containing three kinds of flame retardant additives in various quantities: ammonium polyphosphate (AP423 from Clariant), tetrabromobisphenol A (TBBA), and a system combining TBBA and antimony trioxide (Sb_2O_3). The ratio of TBBA to Sb_2O_3 was fixed to 2.8. This ratio is in the typical range for flame retarded styrenic polymers such as high-impact polystyrene and ABS [11,12]. The compounds were prepared using a Clextral BC21 twin-screw extruder. Squared sheets of thickness 4 mm for cone calorimeter tests were injection-molded using a Sandretto 95-ton press. Processing temperatures were typically fixed to 200 °C.

Thermogravimetric analyses (TGA) were performed using a Pyris-1 Perkin–Elmer apparatus. Samples of 10 (±2) mg were heated under a nitrogen flow at a heating rate equal to 10 °C/min from ambient temperature to 750 °C.

PCFC tests were performed using fire testing technology apparatus (Fig. 1) according to the ASTM D7309 [13]. A sample of 2 (±1) mg was heated under nitrogen flow to 750 °C at a heating rate equal to 1 K/s. Gases are extracted and sent to a combustion chamber in the presence of a N_2/O_2 80/20 flow. The flow rate is fixed to 100 cm^3/min. At this flow rate, the residence time of gases in the combustor is approximately 10 s. All details about the PCFC construction can be found elsewhere [5]. It should be noted that the combustor was designed to ensure complete oxidation of pyrolysis products at a combustion temperature fixed to 900 °C.

For each experiment, the sample weight was chosen carefully to ensure that O_2 is always in excess. The temperature of combustion was monitored between 900 and 600 °C. Combustion efficiency at a temperature T is calculated as follows:

$$\chi(T) = (\Delta O_2 \text{ at the temperature } T)/(\Delta O_2 \text{ at } 900\,^\circ\text{C}), \tag{2A}$$

where ΔO_2 at the temperature T is the mass or volume of oxygen consumed at the combustor set point temperature T, and ΔO_2 at

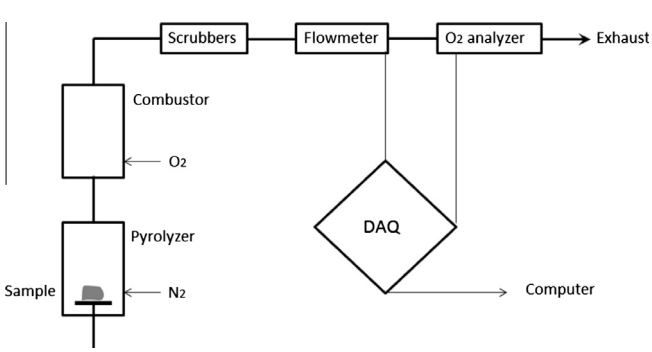

Fig. 1. Schema of pyrolysis–combustion flow calorimeter (from [9]).

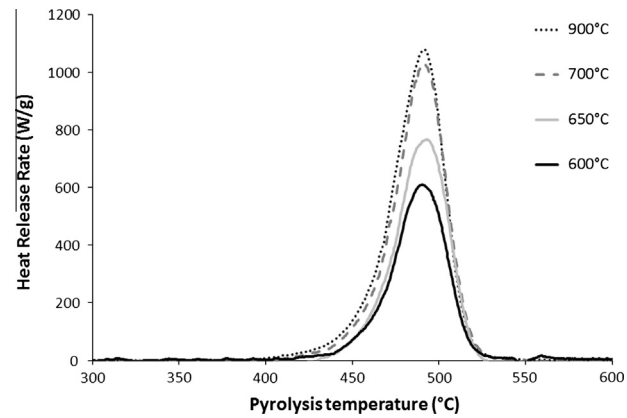

Fig. 2. Heat release rate curves measured by PCFC for LDPE at various combustion temperatures (900, 700, 65, 0 and 600 °C).

900 °C is the oxygen consumed by combustion of the pyrolysis gases at T = 900 °C. As said previously, 900 °C is generally enough to ensure complete combustion.

The heat release rate is calculated from the oxygen consumption according to Huggett's relation (1 kg of consumed oxygen corresponds to 13.1 MJ of released heat) [14]. Total heat release is equal to the area under the curve plotting the heat release rate versus the pyrolysis temperature. Therefore, combustion efficiency is practically calculated as follows:

$$\chi(T) = (\text{total heat release at the temperature } T) / (\text{total heat release at } 900\,^\circ\text{C}). \tag{2B}$$

Eqs. (2A) and (2B) are equivalent in this case.

It should be recalled that the pyrolysis conditions were never changed. Only the combustion efficiency of the gases obtained by pyrolysis was affected when the combustion temperature was modified. As an example, the heat release rate over the whole range of pyrolysis temperatures is given in Fig. 2 for LDPE at various combustion temperatures. While no change could be observed between 900 and 700 °C, the heat release rate decreases significantly below the latter temperature.

Cone calorimeter tests were performed using a FTT apparatus according to the ISO 5660 standard. Irradiance was fixed at 50 kW/m^2. Ignition was piloted using a spark igniter. Only formulations from series B and C were tested (amounts of polystyrenes from series A were insufficient). All formulations were duplicated.

Py–GC/MS analyses were performed with a Pyroprobe 5000 pyrolyzer equipped with a CDS Analytical for flash pyrolysis in a helium environment. The samples were heated to 600 °C. The heating rate was close to 20 °C/ms. For PS-P, an additional experiment was carried out: the sample was heated in two steps, to 400 °C and then to 600 °C. Each temperature was held for 15 s; then the gases were drawn toward the gas chromatograph for 5 min. The Pyroprobe 5000 is interfaced with a Varian 450-GC gas chromatograph. In the oven the initial temperature of 70 °C was raised to 250 °C at 10 °C/min. The column was a Varian Vf-5ms capillary column (30 m × 0.25 mm) and helium (1 mL/min) was used as the carrier gas. The gases were introduced from the GC transfer line to the ion trap analyzer of the Varian 240-MS mass spectrometer through a direct-coupled capillary column. Initial sample weight was less than 1 mg for each experiment.

3. Results and discussion

The main values obtained in the PCFC for all studied materials are listed in Table 2. HRC, THR, and temperature at pHRR are given

Table 2
PCFC results for all tested materials.

Combustion temperature (°C)	HRC (J/g K)	THR (kJ/g)	Temp. at pHRR (°C)	*X*			Isoconversion temperature (°C)
	900 °C	900 °C	900 °C	600 °C	650 °C	700 °C	
Series A							
PS	840	34.7	434	0.21	0.41	0.88	696
PS-CH_3	684	35.8	435	0.17	0.46	0.96	NA
PS-OCH_3	653	29.8	432	0.26	0.48	0.89	NA
PS-Cl	466	23.8	433	0.11	0.30	0.63	NA
PS-Br[a]	190	12.3	424	0.28	0.34	0.66	NA
PS-P		15.5		0.48	0.67	0.93	NA
PS-P first peak	184	10	345	0.54	0.71	0.93	NA
PS-P second peak	155	5.5	487	0.36	0.6	0.93	NA
Series B							
ABS	541	34.1	467	0.32	0.57	0.95	671
PMMA	419	22.8	390	0.40	0.73	0.86	719
PA6	525	28.5	474	0.46	0.71	0.88	NA
PA11	709	31.1	450	0.50	0.77	0.93	717
LDPE	1092	41.1	490	0.57	0.75	0.93	NA
EVA28	751	36.6	483	0.56	0.73	0.84	671
PVC	179	15	463	0.30	0.54	0.65	663
Series C							
ABS 1.6% TBBA	570	32.9	466	NA	0.67	0.90	669
ABS 15.1% TBBA	434	29.7	453	0.25	0.60	0.80	648
ABS 31% TBBA[b]	321	23.8	453	NA	0.59	0.86	640
ABS 1.7% TBBA 0.6% Sb_2O_3	595	36.2	465	0.22	0.67	0.85	683
ABS 4.3% TBBA 1.5% Sb_2O_3	571	32.9	465	NA	0.67	0.92	663
ABS 8.5% TBBA 3% Sb_2O_3	483	30.9	462	0.28	0.62	0.92	644
ABS 13.6% TBBA 4.8% Sb_2O_3	406	27.9	463	0.26	0.65	0.87	627
ABS 18.6% TBBA 4.8% Sb_2O_3[b]	360	26.5	462	0.23	0.58	0.86	623
ABS 3.1% APP	579	32.5	463	NA	0.69	0.94	665
ABS 7.9% APP	548	30.8	460	NA	0.75	0.96	666
ABS 15.7% APP	478	27.5	458	NA	0.81	0.99	666
ABS 31.5% APP	391	23.4	458	0.27	0.69	0.92	664
ABS 40% APP	342	20.6	466	NA	0.78	0.98	663

[a] Incomplete combustion at 900 °C.
[b] Possible incomplete combustion at 900 °C.

for a combustion temperature set to 900 °C. Combustion efficiencies are determined for combustion temperatures set to 600, 650, and 700 °C.

3.1. Combustion efficiency of series A: roles of various chemical groups in the flame inhibition effect

This series was studied to evaluate the effect of various chemical groups grafted onto a polystyrene backbone on the combustion efficiency.

The presence of different groups on the aromatic ring of polystyrene modifies the THR for complete combustion. Indeed, these groups modify the composition of the combustible gaseous phase and change energies released by combustion (Fig. 3). Moreover, for the PS-P sample a high char content (36.3 wt%, measured using thermogravimetric analysis) was obtained and explains the low THR value. For the other functionalized polystyrenes, the char formation was negligible (less than 2.5 wt%).

Figure 4 shows the change in combustion efficiency with combustion temperature for the different functionalized polystyrenes. PS, PS-CH_3, and PS-OCH_3 exhibit a same tendency, with a decrease of combustion efficiency below 725 °C. At 650 °C, the combustion efficiency is similar for these polymers (0.41–0.48). For the PS-Br, sample the decrease of combustion efficiency is observed at higher temperatures (between 750 and 800 °C). The value is stable between 675 and 700 °C (0.65) and decreases further below 675 °C. Nevertheless, it should be noticed that the combustion efficiency curve does not show any plateau at high temperature: therefore, it is not possible to conclude that the combustion is

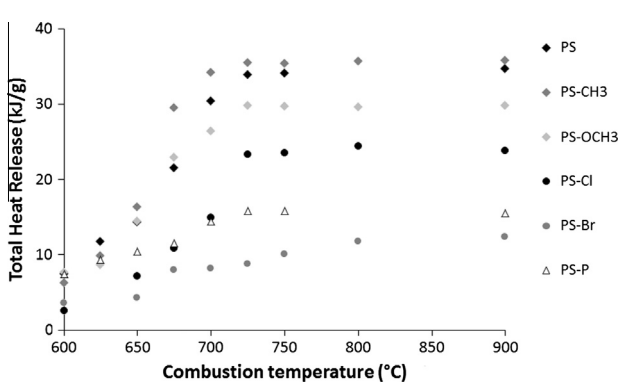

Fig. 3. THR of various functionalized polystyrenes measured by PCFC for different combustion temperatures.

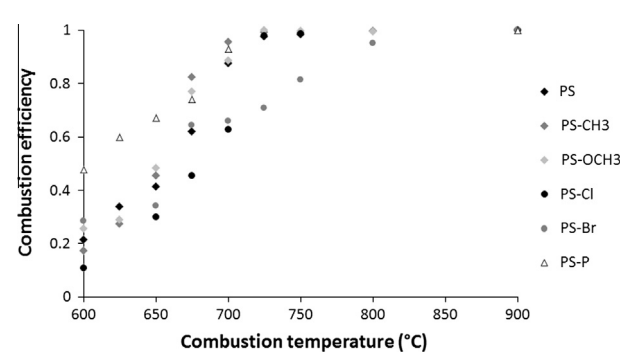

Fig. 4. Combustion efficiency of various polystyrenes measured by PCFC at different combustion temperatures.

complete at 900 °C for PS-Br. A FTIR analysis of gases released after combustion at 900 °C confirms the presence of CO; i.e., some gases are not fully oxidized (data not shown). This result is not in agreement with the work of Lyon and Walters [15], which showed that the oxidation of highly brominated compounds is complete (99%) in 10 s at 900 °C in PCFC. In our case, the combustion efficiency at a lower temperature than 900 °C is overestimated. For the PS-Cl sample, the critical temperature is intermediate (725–750 °C), but this decrease is faster: the combustion efficiency is close to 0.6 at 700 °C, 0.3 at 650 °C, and 0.1 at 600 °C. These results are in agreement with the well-known flame inhibition effect of the halogens. It seems that gases released from pyrolysis of halogenated polymers need a higher temperature for total combustion in presence of oxygen.

Unlike the other modified polystyrenes, PS-P decomposes in several steps. Figure 5 shows the mass loss rate of the different modified polystyrenes measured by thermogravimetric analysis. Figure 6 shows the mass loss rate (measured in TGA) and the heat release rate (measured in PCFC for a combustion temperature of 900 °C) of PS-P. Samples undergo linear heating under nitrogen flow in TGA and PCFC. Therefore the curves are similar in both analyses for the same formulation. Nevertheless the temperature value of the different peaks is slightly shifted between TGA and PCFC analyses because the heating rate is not the same (10 °C/min in thermogravimetric analysis, 60 °C/min in PCFC). It could be considered that PS-P degrades in two main steps: between 150 and 380 °C and between 420 and 570 °C. While the mass loss is similar for both steps (30–33 wt%), the heat release (i.e., the area

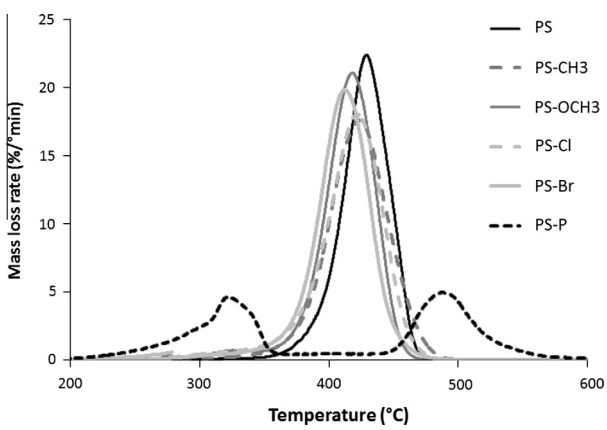

Fig. 5. Mass loss rate of the different polystyrenes measured by thermogravimetric analysis (nitrogen flow, 10 °C/min).

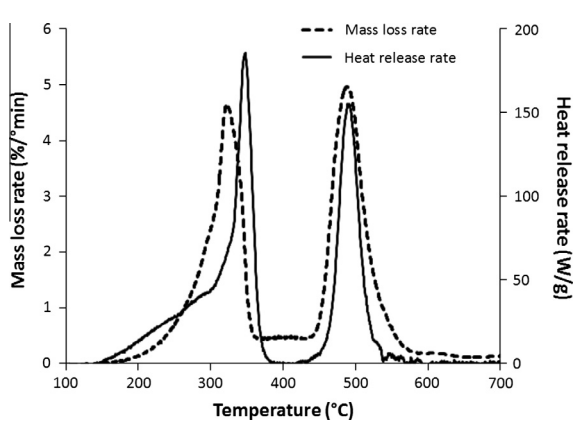

Fig. 6. Mass loss rate and heat release rate (at a combustion temperature 90 °C) of PS-P.

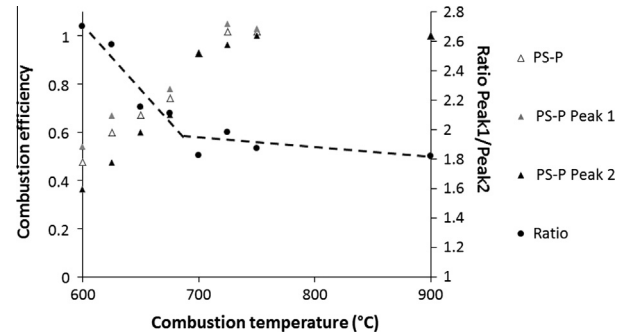

Fig. 7. Combustion efficiency of PS-P, first and second peaks of degradation and ratio between the heat releases of both peaks.

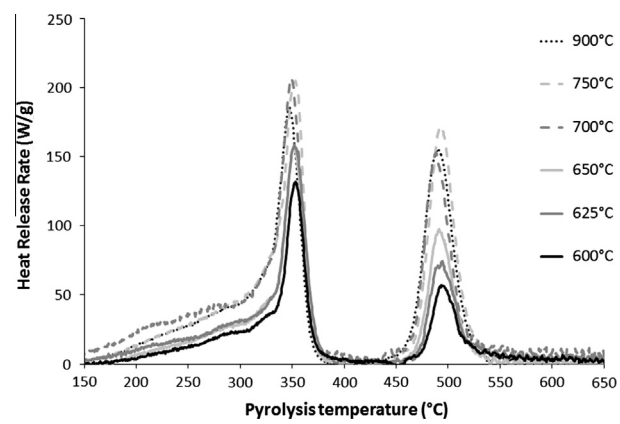

Fig. 8. Heat release rate of PS-P measured by PCFC for various combustion temperatures.

under the peak of heat release rate) is significantly different: 10 kJ/g and 5.5 kJ/g, respectively, for the first and second steps. Therefore, the effective heat of combustion (EHC, defined as the THR divided by the mass loss, i.e., the mass of volatiles released for each step separately) is strongly different for the two steps: 32.5 and 16.9 kJ/g, respectively, for the first and the second steps. This difference is due to the different natures of the released gases during the two steps.

The combustion efficiency of each step of degradation (PS-P peak 1 and PS-P peak 2) was calculated as a function of combustion temperature and compared with the global combustion efficiency of PS-P (Fig. 7). The ratio between the heat releases of the first and second peaks is also shown. The combustion efficiency starts decreasing below 725 °C. The decrease is faster for the second peak and its combustion efficiency is only 0.36 at 600 °C, while the value for the first peak is 0.54 at the same combustion temperature. Therefore, the ratio between the heat release of the two peaks increases progressively from 1.8 to 2.7 when the combustion temperature decreases. The increase of this ratio is due to the gases released during the second step, which need higher temperatures to undergo total oxidation. Figure 8 shows clearly the faster decrease of the heat release corresponding to the second degradation step. This difference of evolution for the two peaks also proves the difference of the gases released by the two degradation steps.

Py–GC/MS analyses (Fig. 9) confirm the previous conclusions. The flash pyrolysis at 600 °C (i.e., at a temperature much higher than the degradation temperature) leads to various gases according to the chemical structure of the polymer. In most cases the molecules formed by pyrolysis of the modified polystyrenes are products of depolymerization. The poly(4-bromostyrene) and the poly(4-chlorostyrene) release large amounts of halogenated

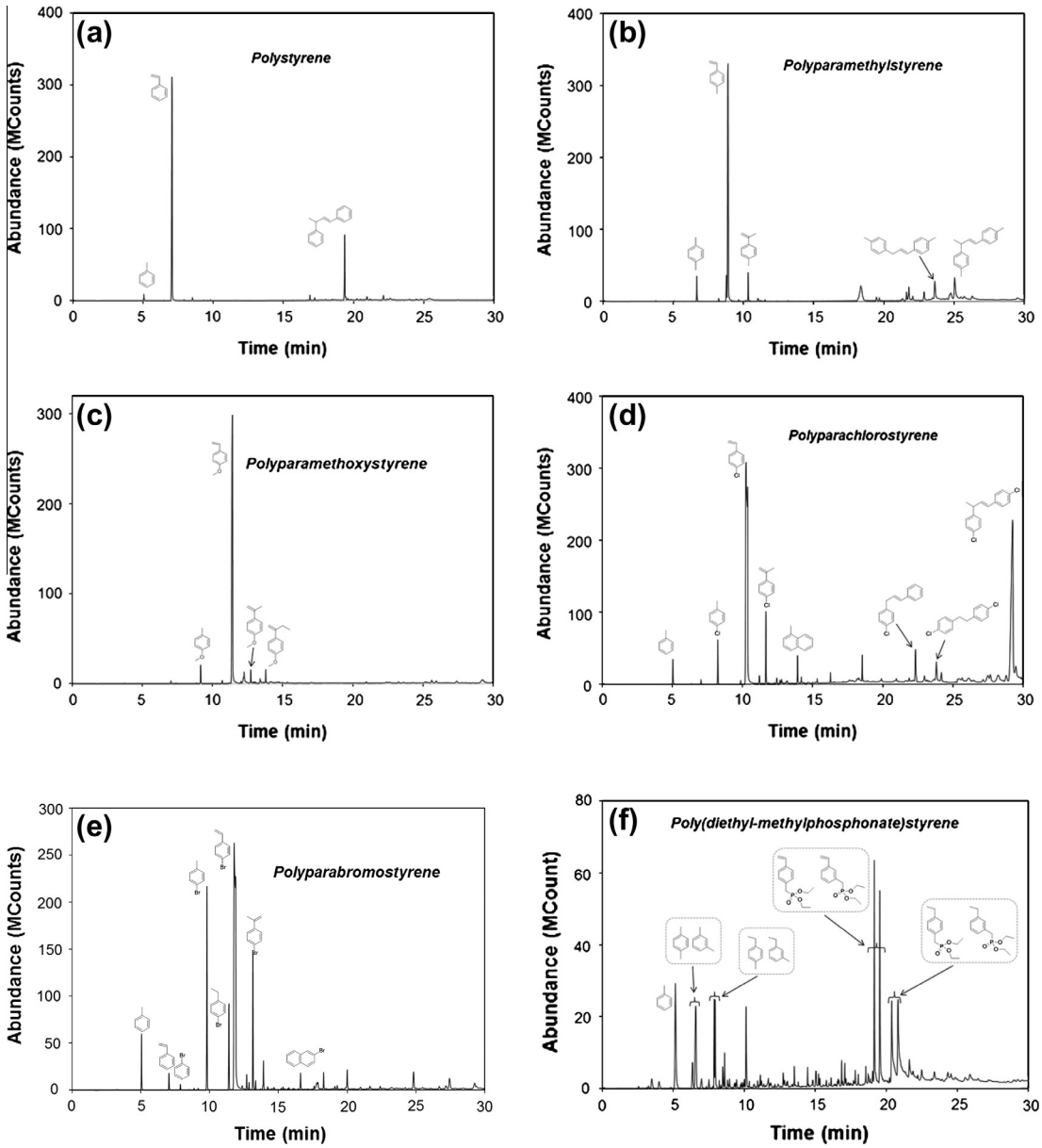

Fig. 9. Py–GC/MS analyses of various modified polystyrenes at 600 °C.

aromatic molecules. It should be recalled that these halogenated polystyrenes need a higher temperature for complete combustion in PCFC. Therefore it can be confirmed that the presence of halogenated groups protects the gases against combustion (flame inhibition effect).

PS-P pyrolysis exhibits a complex spectrum with many peaks, and some of them correspond to products of depolymerization. Phosphonated styrenic molecules with a substitution in the *meta* or *para* position are observed (the phosphonated polystyrene used in this study was obtained by polymerization of a mixture of diethyl 3-vinylbenzylphosphonate and diethyl 4-vinylbenzylphosphonate). Some intensive peaks correspond to aromatic products without phosphorus. It should be noticed also that this phosphonated polystyrene undergoes strong charring. Therefore, it is probable that a significant fraction of the phosphorus remains in the condensed phase. The presence of some phosphonated molecules in the gaseous phase after pyrolysis is not contradictory to the well-accepted mode of action of phosphorus compounds in the condensed phase (char promotion).

It must be kept in mind that the phosphonated polystyrene decomposes in two well-separated steps. A single analysis at 600 °C does not allow the separation of gases released by the two steps. Therefore, Py–GC/MS analyses were performed successively on the same sample at 400 °C (i.e., at a temperature higher than the first step) and then at 600 °C (i.e., at a temperature higher than the second step). According to EHC values and combustion efficiency curves, it was concluded that the composition of gases released during the two steps is significantly different. Figure 10 shows the Py–GC/MS results, which confirm this point. As expected, very different molecules are released during the two steps. During the first step, phosphonated styrenic molecules are the main products released, while nonphosphonated aromatic molecules are released during the second step. This result is in good agreement with Dumitrascu and Howell [16] and Tai et al. [17,18]. In these works, copolymers of styrene and phosphonated styrenes with various structures were synthesized and studied. In many cases, two peaks of decomposition were observed. The first one, at low temperature, was attributed to the decomposition

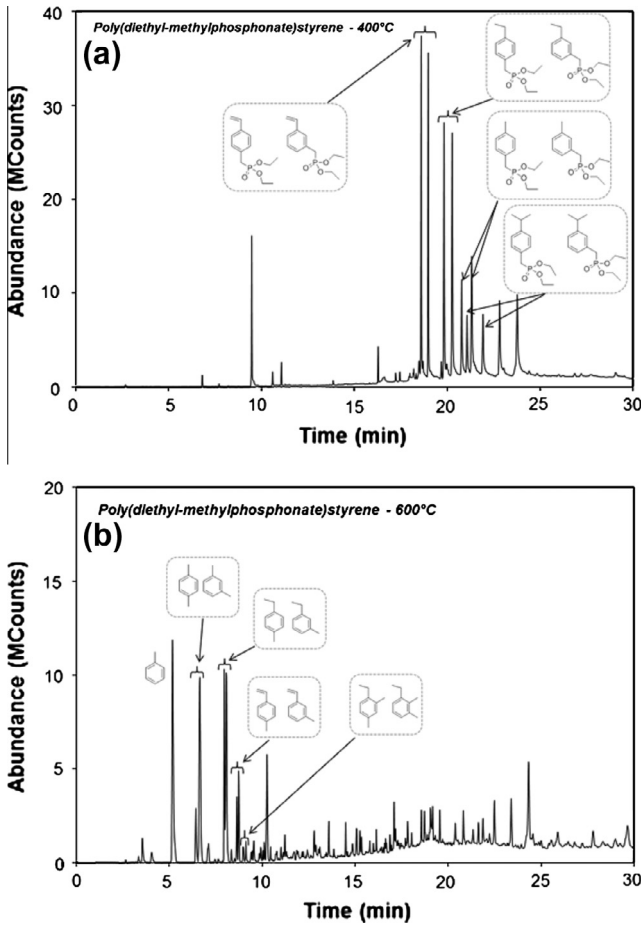

Fig. 10. Py–GC/MS analyses of PS-P at 400 °C (top) and 600 °C (bottom).

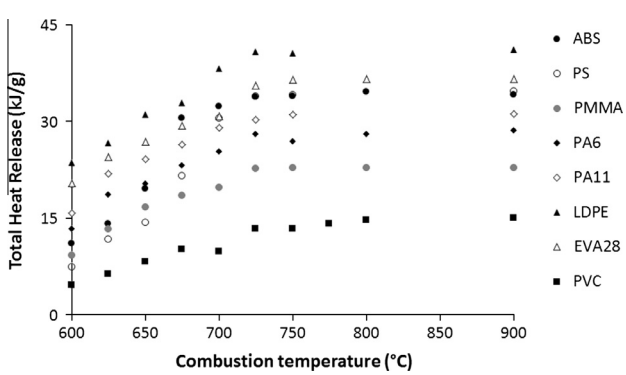

Fig. 11. Total heat release of various commercial polymers measured by PCFC at different combustion temperatures.

of the phosphonated comonomer. This peak was much lower than the one that we observed for PS-P because the content of the phosphonated comonomer was not higher than 20 wt%. In particular, Dumitrascu and Howell have studied a copolymer containing 5–20 wt% of the (diethylmethylphosphonate)styrene. The authors observed a small peak of heat release rate between 300 and 375 °C in PCFC, which was attributed to the release of phosphonate units.

The low EHC associated with the second peak is surprising because the molecules released during this step are toluene, methylstyrene, etc., which should exhibit a much higher effective heat of complete combustion. For example, the effective heat of complete combustion calculated from the atomic composition is 41 kJ/g for toluene (see [19] for a description of the calculation). This result has not been explained yet.

3.2. Combustion efficiency of series B: a phenomenological modeling to describe the combustion of pyrolysis gases

THR of eight commercial polymers measured by PCFC for various combustion temperatures are presented in Fig. 11. The THR for complete combustion is different for all polymers in each case. As previously, Fig. 12 was plotted to study specifically the combustion efficiency. It appears that these polymers could be separated in three groups according to the shape of the combustion efficiency curve. The first group gathers the aliphatic polymers containing C, H, O, and N. These polymers show complete combustion when the combustion temperature is higher than 725 °C. Below this critical temperature, combustion efficiency decreases progressively. Its value is still 0.8 at 675 °C and close to 0.6–0.7 at 625 °C. The second group gathers the styrenic polymers PS and ABS. As for the first group, these polymers exhibit complete combustion above 725 °C. Nevertheless, below this temperature, the combustion efficiency decreases drastically. At 675 °C, its value is 0.6, and it is close to 0.4 at 650 °C. The last group corresponds to PVC, i.e., a halogenated polymer. The curve is more complex and shows two stages, as for PS-Br from series A. Combustion efficiency starts decreasing slowly below 800 °C. At 725 °C, the value is 0.83. Below this temperature, the combustion efficiency decreases faster (close to 0.5 at 650 °C).

Most of the polymers considered undergo degradation in one step during the pyrolysis. Nevertheless, EVA and PVC exhibit two peaks of degradation. As for PS-P, the gases formed during the two degradation steps have different combustion efficiencies. For example, the peak of HRR corresponding to acetic acid released during the first degradation step of EVA totally disappears when the combustion temperature is lower than 600 °C. This observation points out that acetic acid needs a combustion temperature higher than that of the gases released from the second step (pyrolysis of polyenes formed after release of acetic acid). Nevertheless, the THR values associated with the first peak are too low to be measured accurately. Similarly, the THR values associated with the different degradation steps of PVC are too low.

For most of the tested polymers from series A and B, the combustion efficiency curve is relatively simple. The combustion efficiency is equal to 1 above a critical temperature (close to 700 °C) and exhibits a sigmoidal decrease below this temperature. By analogy with crystallization curves (the Avrami model), the equation

$$1 - X(T) = \exp(-A \times T^n), \tag{3}$$

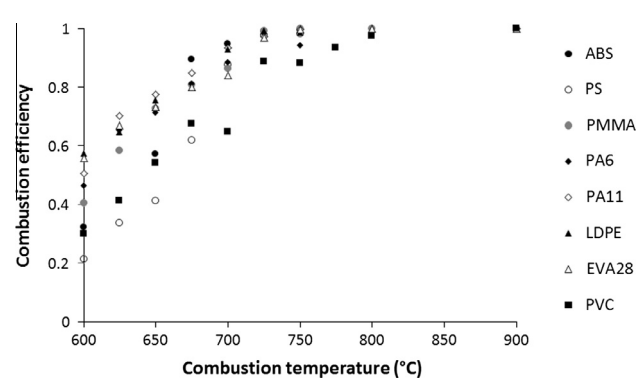

Fig. 12. Combustion efficiency of various commercial polymers measured by PCFC at different combustion temperatures.

was proposed to model the combustion efficiency curves. Plotting $\mathrm{Ln}(-\mathrm{Ln}(1-X(T)))$ versus $\mathrm{Ln}(T)$ makes it possible to determine the two parameters n and A:

$$\mathrm{Ln}(-\mathrm{Ln}(1-X(T))) = n \times \mathrm{Ln}\,T + \mathrm{Ln}A. \quad (4)$$

At least five experimental points between 600 and 750 °C were taken into account to fit these parameters (at higher temperatures, combustion efficiency is too close to 1). Halogenated polymers (PS-Br, PS-Cl, and PVC) were not considered, since their combustion efficiency curves show two stages. Two sets of parameters were calculated for PS-P, corresponding to the first and second pyrolysis steps.

Figure 13 shows graphically the calculation of n and A for PS. For all the samples, the correlation coefficient R^2 is higher than .95 (except for the first pyrolysis peak of PS-P: $R^2 = 0.93$).

Figure 14 shows the variation of n versus LnA for the different polymers studied. Surprisingly, a linear relation between n and LnA is highlighted indicating a strong correlation between both parameters. Presently, no physical sense could be attributed to A and n. Lyon et al. have presented another approach to evaluating the kinetic parameters for the thermal oxidation of fuels in excess of oxygen [15,20,21]. This approach is more valuable since it allows calculating "physical" parameters. But it needs isothermal experiments which are not possible using PCFC. Nevertheless, these results show that the knowledge of n (or alternatively A) is enough to describe precisely the combustion efficiency curve of the polymers under consideration. A high value for the n parameter corresponds to a fast decrease in combustion efficiency below the critical temperature (close to 700 °C). It could be noticed that the calculated parameters are consistent with the chemical structure of the studied polymers. For example, PA6 and PA11 exhibit very similar n and A values. EVA28 and LDPE show the lower n values. Styrenic polymers exhibit also similar parameters (high n values), except PS-P. The parameters for the second peak of this polymer are close to (but lower than) those of styrenic polymers, while

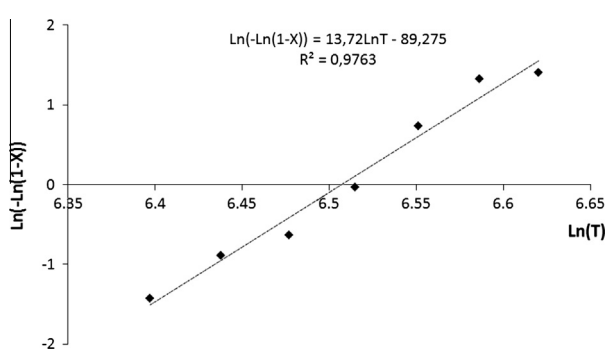

Fig. 13. Calculation of n and A parameters for PS.

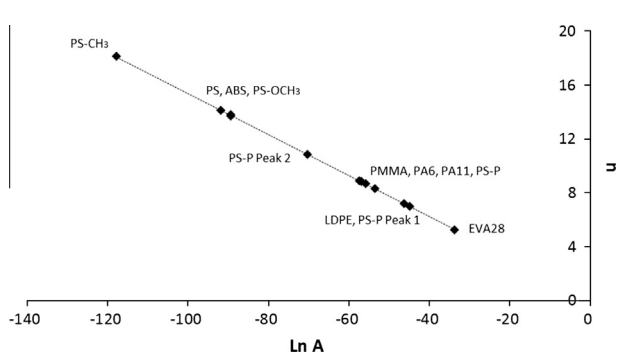

Fig. 14. $n = f\,(\mathrm{Ln}A)$ for the polymers under consideration.

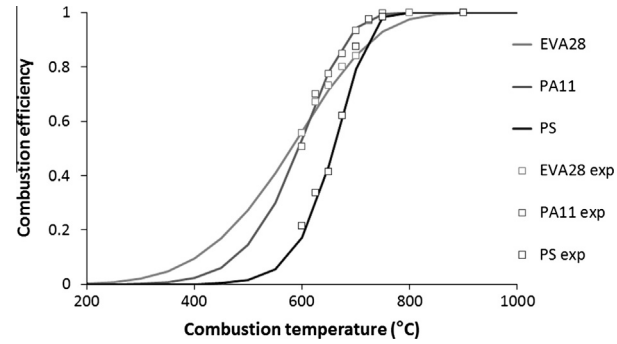

Fig. 15. Modeling curves and experimental data for PA11, PS, and EVA28.

the parameters for the first peak are close to those of LDPE. Very noticeably, this result is in good agreement with Py–GC/MS analyses. Indeed nonsubstituted aromatic molecules are released during the second step of degradation. These molecules are close to those for the molecules released during the polystyrene pyrolysis.

Figure 15 shows the modeling curves for PS, EVA28, and PA11. These curves were drawn from Eq. (1) and the parameters n and A calculated previously. Experimental points are also plotted for these three polymers. Very good agreement has been obtained between the modeling curve and experimental points in the three cases. These curves should be very useful in understanding some phenomena as ignition. Ignition occurs when fuels can be oxidized in the gaseous phase. This oxidation requires oxygen and heat. According to Fig. 15, it appears that a very low temperature (400 °C) is sufficient to start the combustion of a significant amount of the gases released by the pyrolysis of EVA28. Combustion efficiency is equal to 0.1 at this temperature. In contrast, a higher temperature (550 °C) is required to allow similar combustion efficiency for PS. While all gases released by PS are burnt at 700 °C, the combustion efficiency of EVA28 is not equal to 1 at this temperature (according to the modeling curve, but experimental combustion efficiency is closer to 1 in this case). Similar inversion could be observed between EVA28 and PA11 curves but at lower temperature (inversion point is close to 600 °C). In contrast, when PS and PA11 curves are compared, combustion efficiency is higher for PA11 whatever the temperature.

3.3. Combustion efficiency of series C: correlations between PCFC and cone calorimeter tests

Series C was tested to evaluate the flame inhibition when the flame retardants were not grafted onto the macromolecular backbone but physically incorporated into the matrix. Moreover, these formulations (and some polymers from series B) were tested with a cone calorimeter apparatus to identify possible correlations between PCFC and cone calorimeter results. Three flame retardant systems were studied: TBBA, TBBA/Sb_2O_3, and APP. TBBA is known as a flame retardant acting in the gaseous phase. Synergy between TBBA and antimony trioxide is also well known. APP is a flame retardant acting in the condensed phase as a charring promoter. Moreover, the release of ammonia from APP also leads to a dilution of the gaseous phase. Flame inhibition is not considered as one of the modes of action of this additive, but it was reported that some phosphorus compounds could act as flame inhibitors. Braun et al. [22] has studied the flame retardancy of epoxy resins containing phosphine oxide, phosphinate, phosphonate, and phosphate in their structure. The authors concluded that phosphorus compounds (particularly phosphine oxide) also act as flame inhibitors. Nevertheless, their conclusions were based on the decrease in EHC in the cone calorimeter when these compounds were incorporated.

EHC could be reduced not only because of a decrease in combustion efficiency but also because phosphorus gases release intrinsically less heat even if the combustion is complete. Hergenrother et al. [23] studied similar epoxy resins with curing agents containing phosphorus. Combustion efficiency was calculated as the ratio between EHC in fire calorimeter tests and EHC calculated in PCFC at a combustion temperature of 900 °C. Combustion efficiency was found to be 0.7 without phosphorus. Almost all phosphorus-containing samples exhibited higher combustion efficiency. But three samples exhibited significantly lower combustion efficiency (0.55–0.6). In a comprehensive review [24], Schartel noted the flame inhibition of aluminum tris-diethylphosphinate ($AlPO_2$) in PBT/GF (glass fiber) composites. This assertion is based on the calculation of combustion efficiency. The combustion efficiency of PBT/GF is 0.98. The incorporation of 6.3 wt% of $AlPO_2$ decreases this value to 0.64.

Figures 16–18 show the combustion efficiency of ABS filled with TBBA, TBBA/Sb_2O_3, and APP. ABS filled with TBBA exhibits a combustion efficiency curve similar to that of PS-Br (Fig. 16). Combustion efficiency starts decreasing at 800 °C, in particular when high amounts of TBBA are incorporated. At 725 °C, combustion efficiency is decreased to 0.8–0.85, while ABS shows complete combustion in the absence of TBBA. However, at a low combustion temperature (650 °C or lower), no great difference is observed. It should be noted that combustion efficiency is lower for ABS filled with 15.6 wt% of TBBA than for ABS filled with 31 wt% of TBBA (in particular between 675 and 725 °C). A simple explanation is as follows: The combustion efficiency curve of ABS filled with 31 wt% of TBBA does not exhibit any plateau at high combustion temperature, which could indicate that the combustion is not complete even at 900 °C, as for PS-Br. But this result may also be consistent with the saturation effect of the chemical component of flame inhibition when the content of the flame retardant increases [2,3]. At the same time, smaller amounts of fuels are released because TBBA partially replaces ABS. The combination of these two tendencies leads to the increase of combustion efficiency. Nevertheless, total heat release is lower for ABS filled with 31 wt% of TBBA because of the smaller amount of fuels (23.8 and 18.8 kJ/g at 900 and 675 °C for 31 wt% of TBBA versus 29.7 and 20.9 kJ/g at the same temperatures for 15.6 wt% of TBBA). The measurement of the combustion efficiency in PCFC appears as a useful method of optimizing the flame inhibition effect of a flame retardant.

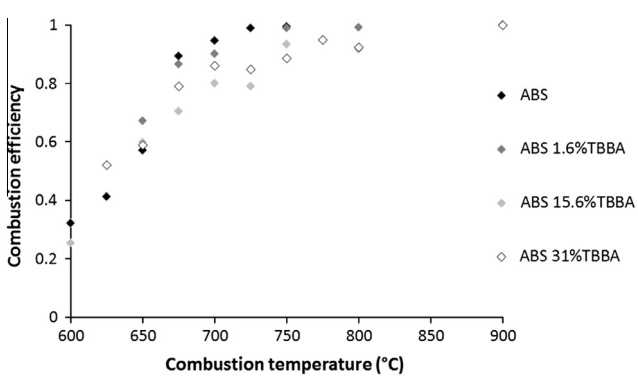

Fig. 16. Combustion efficiency of ABS filled with TBBA measured in PCFC at different combustion temperatures.

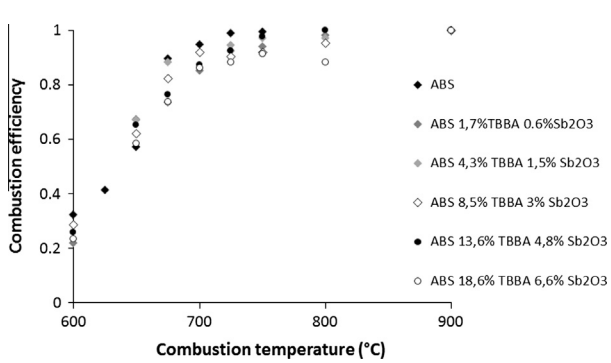

Fig. 17. Combustion efficiency of ABS filled with TBBA and Sb_2O_3 measured in PCFC at different combustion temperatures.

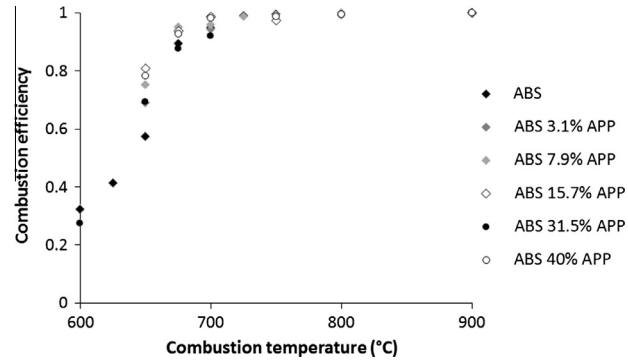

Fig. 18. Combustion efficiency of ABS filled with APP measured in PCFC at different combustion temperatures.

The combustion efficiency of ABS filled with the system TBBA/Sb_2O_3 is also lower than that of pure ABS in the temperature range 675–800 °C (Fig. 17). As reported previously for PS-Br and ABS filled with 31 wt% TBBA, it should be noted that the combustion of ABS filled with 18.6 wt% TBBA and 6.6 wt% Sb_2O_3 may be not complete while the curve does not exhibit any plateau at high combustion temperature. As for TBBA, combustion efficiency of all formulations with TBBA/Sb_2O_3 seems to be similar below 650 °C. It should be noted that combustion efficiency is higher for TBBA/Sb_2O_3 than for TBBA at similar FR content (TBBA content is lower in the TBBA/Sb_2O_3 system because of its partial replacement by Sb_2O_3). The synergy between TBBA and Sb_2O_3 does not seem relevant according to these data. Antimony trioxide is believed to enhance the flame inhibition by decomposing and volatilizing bromine compounds at lower temperatures [12,25]. Many works report that antimony trioxide leads to a two-step decomposition in brominated styrenic polymers [25,26]. Jakab et al. [25] identified that the first step, at low temperature, corresponds to the release of $SbBr_3$, brominated organic compounds, water, and styrene (the studied matrix was hiPS). In PCFC, this step should hardly be detected, since most of the gases are not (or are little) combustible. Indeed, we observed a small shoulder below 400 °C for some ABS containing sufficient amounts of TBBA/Sb_2O_3 (not shown). This shoulder was also observed without a synergist, but to a smaller extent. Flame inhibition from bromine should be most efficient if bromine is released during the decomposition of ABS. While the sample is heated according to a linear heating rate in PCFC, maybe bromine is volatilized too early in the presence of antimony trioxide, and its efficiency is decreased.

Whatever the APP content in ABS, no decrease in combustion efficiency is observed (Fig. 18). Combustion efficiency is very close to the value for pure ABS above 675 °C. Moreover, below this temperature, combustion efficiency seems to be higher for ABS filled with APP. This behavior could not be explained clearly. This may be due to measurement uncertainties. But it could be remarked that PS-P also exhibits significantly higher combustion efficiency at low temperature than other modified polystyrenes. In all cases, the results show clearly that APP does not exhibit any flame inhibition action.

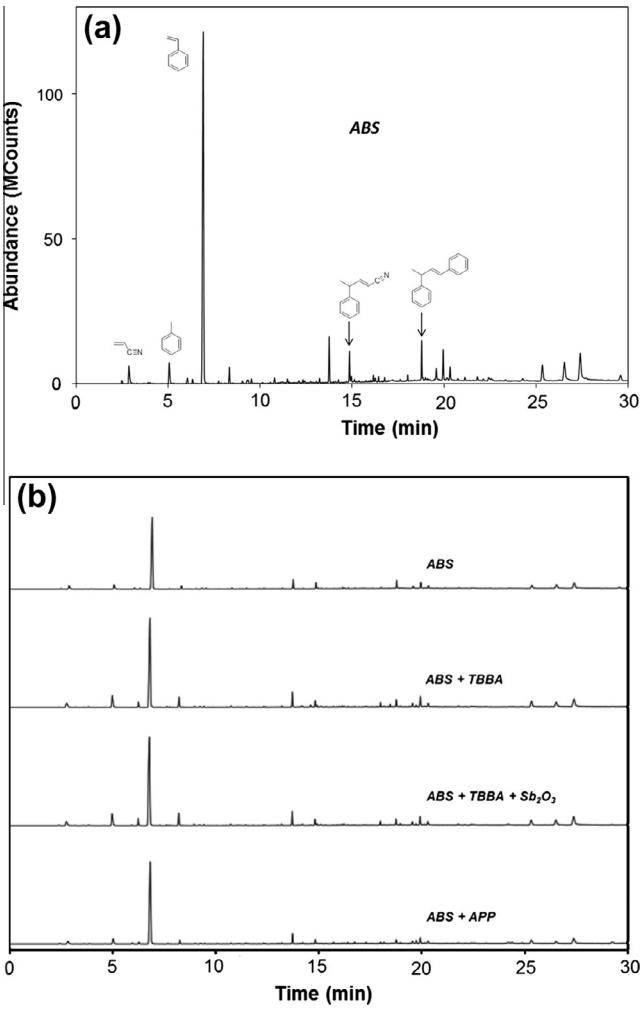

Fig. 19. Py–GC/MS analyses of pure and flame retarded ABS at 600 °C.

Py–GC/MS analyses were performed on ABS and ABS filled with 31.5 wt% of APP (10 wt% of P), 17 wt% of TBBA (10 wt% of Br), and 8.5 wt% of TBBA with 3 wt% of Sb_2O_3 (5 wt% of Br) to evaluate the changes in the gaseous phase (Fig. 19). Products from pyrolysis of styrenic polymers containing brominated flame retardants with and without antimony trioxide have been extensively studied [25,27,28]. Many brominated compounds are released, but the Py–GC/MS chromatogram is dominated by the products from the decomposition of the matrix [25]. The accurate study of the pyrolysis products is out of the scope of this article, but it is clear from Fig. 19 that the decomposition of the ABS matrix is not (or is little) modified when flame retardants are incorporated. This result confirms that the combustion efficiency in the presence of TBBA does not decrease, because the gases released from pyrolysis would be different in nature (and would exhibit another combustion efficiency profile). The combustion efficiency could be attributed to flame inhibition (or flame poisoning). This flame inhibition occurs when HBr from debromination of TBBA reacts with highly reactive radicals OH· to form more stable radicals. While OH· radicals are involved in the oxidation mechanism of fuels, their trapping leads to incomplete combustion.

Correlations between the cone calorimeter and the PCFC are still a challenge. As explained in the Introduction, three reasons could lead to noncorrelated results between the two experimental techniques. Combustion efficiency is one of these reasons, since the PCFC test is generally performed at a high combustion temperature (900 °C), which ensures complete combustion. In contrast, combustion conditions are not controlled during a cone calorimeter test, and therefore combustion efficiency could only be calculated a posteriori. Flame retarded ABS and some polymers from series B were tested in a cone calorimeter test at irradiance equal to 50 kW/m^2. The combustion efficiency in the cone calorimeter could be calculated using the equation

$$\chi(T) = (\Delta O_2(\text{cone}))/(\Delta O_2(\text{PCFC at } 900\,^\circ\text{C})), \tag{5A}$$

where ΔO_2 (cone)T is the mass or volume of oxygen consumed during cone calorimeter test T, and ΔO_2 (PCFC at 900 °C) is the oxygen consumed by complete combustion of the pyrolysis gases at T = 900 °C in the PCFC.

Heat release is measured in the cone calorimeter according to the oxygen depletion method. Therefore we calculated the combustion efficiency using the equation

$$\chi(\text{cone}) = (\text{THR}(\text{cone}))/(\text{THR}(\text{PCFC at } 900\,^\circ\text{C})), \tag{5B}$$

which is equivalent to Eq. (5A). THR in the cone calorimeter is usually calculated in MJ/m^2. Knowing the surface area and the initial mass of the sample, THR could easily be calculated in kJ/g (as in Eq. (5B)). It should be also noticed that mass residues in the cone and in the PCFC are similar in most cases. Discrepancy is observed only when polymers or fillers with high thermal stability are not fully degraded in the cone calorimeter [7]. That is not the case here. Discrepancy could also occur when char undergoes thermo-oxidation, mainly after flame-out [29]. But in this study, THR at flame-out has been considered. Therefore, the combustion efficiency calculated according to Eq. (3) is very close to the combustion efficiency calculated considering EHC (we have checked that the two methods lead to similar values of combustion efficiency).

Isoconversion temperature was defined as the combustion temperature in the PCFC needed to obtain the same combustion efficiency as in the cone calorimeter test. In each case, its value was calculated by linear interpolation between two experimental measurements in PCFC. Figure 20 shows the evolution of the isoconversion temperature versus the combustion efficiency in cone calorimeter. Surprisingly most of the formulations exhibit close values for isoconversion temperature (between 650 and 700 °C). Moreover, a rough tendency could be drawn between this parameter and the combustion efficiency. For low combustion efficiency, the isoconversion temperature is lower than 650 °C (between 630 and 650 °C). For high combustion efficiency (close to 1), the isoconversion temperature could increase to 720 °C. Of course the combustion conditions are very different between the cone calorimeter and the PCFC. The temperature of the diffusion flame in the cone calorimeter is 1800–2000 K and the residence time of gases in this flame is on the order of milliseconds. In the PCFC,

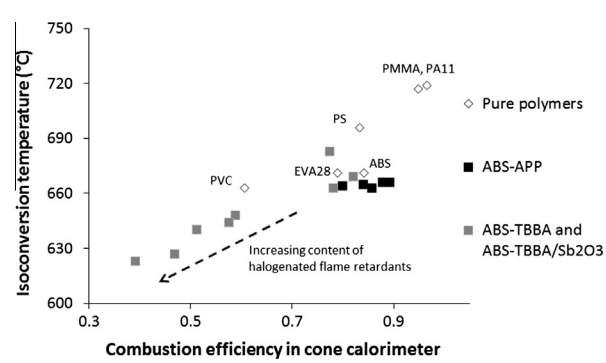

Fig. 20. Isoconversion temperature versus combustion efficiency in the cone calorimeter (irradiance 50 kW/m^2) for flame retarded ABS and pure polymers.

the thermal oxidation occurs under premixed nonflaming conditions and the residence time of gases in the combustor is close to 10 s (as said in the Experimental section). Therefore the isoconversion temperature is only a parameter that allows comparing cone calorimeter and PCFC results. It is not the true temperature of the combustion zone in the cone calorimeter.

It could be noted that the isoconversion temperature does not change when APP is incorporated into ABS. In contrast, the addition of TBBA or TBBA/Sb_2O_3 leads to a decrease in combustion efficiency and isoconversion temperature. PVC, as a halogenated polymer, exhibits also a relatively low isoconversion temperature, in comparison to other pure polymers.

Our results also allow prediction of the combustion efficiency in the cone calorimeter test using PCFC tests. Two analyses at combustion temperatures equal to 650 and 700 °C allow determining the lower and the upper limits of combustion efficiency. Nevertheless, in this range, combustion efficiency could change drastically for many formulations, and therefore the prediction is not so precise. For example, these lower and upper limits are 0.41 and 0.88, respectively, for PS. In contrast, for PA6, the lower and upper limits are 0.72 and 0.88, respectively, which allows quite a good prediction.

The peak of the heat release rate at the isoconversion temperature in the PCFC was calculated for all flame-retarded ABS. As for the isoconversion temperature, these data were determined by linear interpolation between two experimental pHRR (for example, the pHRR at an isoconversion temperature equal to 660 °C was calculated by interpolation between pHRR measured at 650 and 675 °C). All formulations were decomposed in one step. In some cases, a very small shoulder at low temperature was observed. This shoulder was neglected. In a previous work [30], an empirical method was proposed for comparing cone calorimeter and PCFC data. Two parameters were defined as follows:

$$R1 = (\text{pHRR(flame retarded polymer) in the PCFC})/(\text{pHRR(pure polymer) in the PCFC}), \quad (6)$$

$$R2 = (\text{pHRR(flame retarded polymer) in the cone calorimeter})/(\text{pHRR(pure polymer) in the cone calorimeter}). \quad (7)$$

According to many experimental results, $R1$ is always equal to or higher than $R2$. This means that the decrease in pHRR is always stronger in the cone calorimeter than in the PCFC when a flame retardant is incorporated. Indeed, in the PCFC, very small samples (with a weight as low as 2 mg) are tested. Therefore, the barrier effect is negligible because no insulating thick layer could be formed. We proposed that the barrier effect is not a significant mode of action of a flame retardant additive when $R1 = R2$. In contrast, when $R2 < R1$ (i.e., when the decrease in pHRR is stronger in the cone calorimeter than in the PCFC), it could be concluded that the barrier effect is efficient in the cone calorimeter. In this first work, PCFC analyses were performed under standard conditions (combustion temperature equal to 900 °C). Of course, this empirical approach is only possible if the thermal stabilities in the PCFC and the combustion efficiencies in the cone calorimeter of both pure and flame retarded polymers (the two other sources of noncorrelation between the cone calorimeter and the PCFC) are similar. These conditions were fulfilled. More details and examples could be found elsewhere [30–33].

Figure 21 shows this $R1$–$R2$ graph for flame-retarded ABS at two combustion temperatures in the PCFC: 900 °C and the isoconversion temperature (this temperature was calculated for each formulation). In the case of ABS filled with APP, $R2$ is lower than $R1$ for both temperatures. The fact that $R2$ is lower than $R1$ is typical of a barrier effect. In this case the barrier is due to the char formed in the presence of the phosphorus compound. $R2$ is lower than

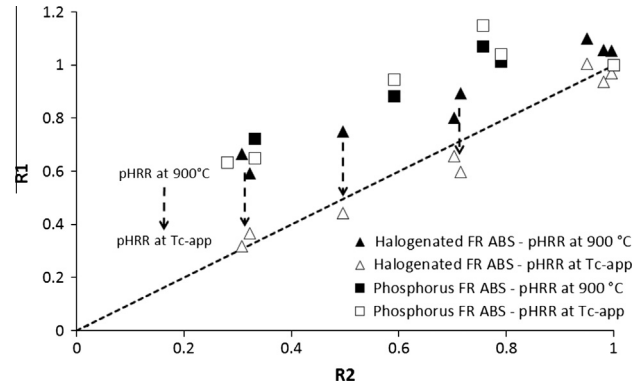

Fig. 21. $R1$–$R2$ graph for flame-retarded ABS at two combustion temperatures in the PCFC.

$R1$ for both combustion temperatures because the combustion efficiency curves are similar for ABS and ABS filled with APP. Therefore, the ratio between $R1$ and $R2$ is the same whatever the combustion temperature in the PCFC.

In contrast, for ABS filled with brominated compounds, $R2$ was lower than $R1$ when PCFC analyses were performed at 900 °C. According to our previous analysis, this would mean that these flame-retarded ABS formulations exhibit a barrier effect, while no residue was formed in the cone calorimeter. Of course this conclusion is wrong. The reason is that these formulations exhibited very different combustion efficiencies in the cone calorimeter test and these differences could not be taken into account in the PCFC when the combustion was complete (at 900 °C). When PCFC analyses were performed at the isoconversion temperature, $R2$ becomes much closer to $R1$ and the barrier effect vanished (as shown by the plotted arrows in Fig. 21). Since the decrease of pHRR is similar in the cone calorimeter and the PCFC in the absence of a barrier effect, it should be possible to predict the pHRR of a flame-retarded formulation in the cone calorimeter test using PCFC if the isoconversion temperature is known. It must be recalled that this temperature seems to range between 650 and 700 °C in most cases.

4. Conclusions

In this article, a new method was proposed for studying the flame inhibition effect of a flame retardant reactive or additive compound using PCFC. The flame inhibition effect of chlorinated and brominated compounds was confirmed, since the combustion efficiency decreases from 750–800 °C for polymers containing these elements. In contrast, other formulations exhibit combustion efficiency close to 1 up to 700–725 °C. PCFC appears as a useful method to optimize the flame inhibition effect of a flame retardant, since very small amounts of sample are needed and combustion conditions can be monitored perfectly. Nevertheless, for some halogenated polymers, the combustion could be not complete at 900 °C. In this case, the method leads to overestimation of the combustion efficiency at any temperature lower than 900 °C.

A phenomenological equation was proposed to model the combustion efficiency versus the temperature of combustion. Only one parameter seems necessary to describe the combustion efficiency curves of the nonhalogenated formulations. For halogenated formulations, at least two steps were observed, and correct modeling needs more experimental points.

Correlations between the cone calorimeter and the PCFC were established. In particular, a new parameter called "isoconversion temperature" was defined. Its value is found close to 650–700 °C for most of the tested formulations, even if the combustion effi-

ciencies in the cone calorimeter test are very different. To evaluate the effective heat of combustion in the cone calorimeter using the PCFC, carrying out the PCFC test in the combustion temperature range 650–700 °C is recommended. Indeed, some pure polymers (such as PVC) could exhibit a relatively low combustion efficiency in the cone calorimeter, and therefore a PCFC test at 900 °C should overestimate the effective heat of combustion significantly. But unfortunately, the combustion efficiency changes strongly in this temperature range. Therefore the prediction of the combustion efficiency in the cone calorimeter using the PCFC could not be accurate.

Moreover, when no barrier effect is efficient, the decrease of pHRR in the cone calorimeter when a flame retardant additive is incorporated could be predicted according to the decrease of pHRR in the PCFC. In this case, PCFC analysis should be carried out at a combustion temperature corresponding to the isoconversion temperature when the flame retardant has a flame inhibition action (such as halogenated additives).

Finally, our results also confirm that the PCFC is a powerful tool for studying various aspects of the flammability of a polymer.

Acknowledgment

We thank Claire Negrell-Guirao from IAM-Institut C. Gerhardt (Montpellier) for providing the PS-P sample.

References

[1] V. Babushok, W. Tsang, Combust. Flame 123 (2000) 488–506.
[2] T. Noto, V. Babushok, D.R. Burgess Jr., Hamins A, Tsang W, A. Miziolek, in: 26th Symposium on Combustion/The Combustion Institute, 1996, pp. 1377–1383.
[3] T. Noto, V. Babushok, A. Hamins, W. Tsang, Combust. Flame 112 (1998) 147–160.
[4] V. Babushok, W. Tsang, G.T. Linteris, D. Reinelt, Combust. Flame 115 (1998) 551–560.
[5] R.E. Lyon, R.N. Walters, J. Anal. Appl. Pyrol. 71 (2004) 27–46.
[6] A.B. Morgan, M. Galaska, Polym. Adv. Technol. 19 (2008) 530–546.
[7] J.M. Cogen, T.S. Lin, R.E. Lyon, Fire Mater. 33 (2009) 33–50.
[8] H. Lu, C.A. Wilkie, Polym. Degrad. Stab. 95 (2010) 564–571.
[9] R.E. Lyon, R.N. Walters, S.I. Stoliarov, Polym. Eng. Sci. 47 (2007) 1501–1510.
[10] B. Schartel, K.H. Pawlowski, R.E. Lyon, Thermochim. Acta 462 (2007) 1–14.
[11] I. Finberg, Y. Bar Yaakov, P. Georlette, Polym. Degrad. Stab. 64 (1999) 465–470.
[12] J. Kaspersma, C. Doumen, S. Munro, A.M. Prins, Polym. Degrad. Stab. 77 (2002) 325–331.
[13] ASTM D7309, 2011.
[14] C. Huggett, Fire Mater. 4 (1980) 61–65.
[15] R.E. Lyon, R.N. Walters, in: Fire and Materials Conference, San Francisco, CA, January 28–30, 2013.
[16] A. Dumitrascu, B.A. Howell, Polym. Degrad. Stab. 96 (2011) 342–349.
[17] Q. Tai, L. Chen, L. Song, S. Nie, Y. Hu, R.K.K. Yuen, Polym. Degrad. Stab. 95 (2010) 830–836.
[18] Q. Tai, L. Song, Y. Hu, R.K.K. Yuen, H. Feng, Y. Tao, Mater. Chem. Phys. 134 (2012) 163–169.
[19] R.N. Walters, S.M. Hackett, R.E. Lyon, Fire Mater. 24 (2000) 245–252.
[20] R.E. Lyon, R.N. Walters, S.I. Stoliarov, J. ASTM Int. 3 (4) (2006) 1–18.
[21] R.N. Walters, R.E. Lyon, in: 40th Meeting of the North American Thermal Analysis Society, Orlando, FL, August 12–15, 2012.
[22] U. Braun, A.I. Balabanovitch, B. Schartel, U. Knoll, J. Artner, M. Ciesielski, M. Doring, R. Perez, J.K.W. Sandler, V. Altstadt, T. Hoffmann, D. Pospiech, Polymer 47 (2006) 8495–8508.
[23] P.M. Hergenrother, C.M. Thompson, J.G. Smith Jr., J.W. Connell, J.A. Hinkley, R.E. Lyon, R. Moulton, Polymer 46 (2005) 5012–5024.
[24] B. Schartel, Materials 3 (2010) 4710–4745.
[25] E. Jakab, Md.A. Uddin, T. Bhaskar, Y. Sakata, Y. Sakata, J. Anal. Appl. Pyrolysis 68–69 (2003) 83–99.
[26] G. Grause, J. Ishibashi, T. Kameda, T. Bhaskar, T. Yoshioka, Polym. Degrad. Stab. 95 (2010) 1129–1137.
[27] G. Grause, D. Karatika, J. Ishibashi, T. Kameda, T. Bhaskar, T. Yoshioka, Chemosphere 85 (2011) 368–373.
[28] S.H. Peng, L.Q. Chen, L.B. Li, M.Q. Xie, Proc. Eng. 11 (2011) 349–354.
[29] R.N. Walters, R.E. Lyon, Fire Mater. 27 (2003) 183–194.
[30] R. Sonnier, L. Ferry, C. Longuet, F. Laoutid, F. Friederich, A. Laachachi, J.M. Lopez-Cuesta, Polym. Adv. Technol. 22 (2011) 1091–1099.
[31] L. Tibiletti, C. Longuet, L. Ferry, P. Coutelen, A. Mas, J.J. Robin, J.M. Lopez-Cuesta, Polym. Degrad. Stab. 96 (2011) 67–75.
[32] Y. Quach, N. Cinausero, R. Sonnier, C. Longuet, J.M. Lopez-Cuesta, Fire Mater., in press. doi:http://dx.doi.org/10/1002/fam.1119.
[33] B. Friederich, A. Laachachi, R. Sonnier, M. Ferriol, M. Cochez, V. Toniazzo, D. Ruch, Polym. Adv. Technol., in press. doi:http://dx.doi.org/10/1002/pat.2056.